Received 30 April 2023; revised 24 July 2023; accepted 22 August 2023.
Date of publication 28 August 2023; date of current version 13 September 2023.

Digital Object Identifier 10.1109/OJUFFC.2023.3308553

Mean Radiation Force of Shear Plane Waves on a Sphere in an Elastic Medium

F. G. MITRI (Senior Member, IEEE)
Schlumberger Doll—Research Center, Cambridge, MA 02139 USA
e-mail: f.g.mitri@ieee.org

In Memoriam of Dr. Guillermo C. Gaunaurd (1940–2021), former Associate Editor of IEEE TRANSACTIONS ON ULTRASONICS, FERROELECTRICS, AND FREQUENCY CONTROL, IEEE Fellow, and Senior Physicist.

ABSTRACT The mean (time-averaged) longitudinal force component (i.e. acting along the direction of wave propagation) arising from the interaction of linearly-polarized plane progressive shear elastic waves, incident upon a sphere embedded in an elastic medium, is considered. Exact partial-wave series expansions are derived based on the integration of the radial component of the time-averaged elastodynamic Poynting vector in spherical coordinates. The method is verified stemming from the law of energy conservation applied to elastic scattering. The analytical modeling is useful and provides improved physical understanding of shear-to-compressional (S $\longrightarrow$ P) mode conversion, as well as shear-to-shear (S $\longrightarrow$ S) and transverse-to-transverse (T $\longrightarrow$ T) mode preservation in the context of the mean elastic force. The elastic wave scattering formulation based on Debye's shear and transverse potentials is solved first, and used subsequently to derive the mathematical expression of the mean force efficiency. Numerical computations illustrate the analysis with particular emphasis on the components related to mode preservation, coupling and conversion separately. It is shown here that the total force originates from individual interactions of scattering terms between the scattered pure shear (S $\longrightarrow$ S) and transverse (T $\longrightarrow$ T) waves, in addition to shear-to-transverse (S $\rightleftarrows$ T) coupling, and a shear-to-compression (S $\longrightarrow$ P) mode conversion that contributes negligibly to the total mean force. The benchmark solution presented in this analysis for the time-averaged elastic force of shear plane progressive waves can be utilized to validate numerical methods (such as the FEM, BEM, FDTD or other). The results can provide *a priori* information for the optimization and design of experimental setups in various applications in biomedical ultrasound, elastography and elasticity imaging, shear-wave activation of implantable devices, characterization of biological tissue, seismology and other related applications in elastic wave scattering and radiation force.

INDEX TERMS Mean acousto-elastic force, linearly-polarized shear elastic plane waves, elastic scattering, elastic sphere, linear elasticity, elastodynamic poynting vector (power flow density).

I. INTRODUCTION

SHEAR waves [1] propagating in an elastic solid and scattered by an inclusion provide useful information in various areas in geophysics and the study of seismic waves [2], materials science and nondestructive testing [3], [4], [5], biomedical ultrasound [6], [7], [8], [9], elastography [10] and elasticity imaging [11] to characterize biological tissue [12] to name a few examples.

When an incident shear wave-field interacts with an inclusion [13] (Fig. 1), mode conversion occurs [14], [15], [16], [17], [18], [19], [20], [21], [22], [23], [24], [25], [26] such that compressional (in addition to shear and transverse) scattered waves are generated in the elastic medium of wave propagation [27], [28]. Elastic resonances arise during the scattering process, however, mode conversion/preservation is dictated by an exact set of physical rules that can be understood in terms of polarization [29]. In essence, an incident shear wave-field of plane progressive waves (composed of both S and T waves originating from Debye's shear and transverse potentials) only scatters mode-converted waves S $\rightarrow$ P, while the remaining are mode-preserved S $\rightarrow$ S and T $\rightarrow$ T scattered waves [29], [30] that are uncoupled in linear elastic scattering. Due to the elastodynamic linear momentum transfer from a time-harmonic incident shear wavefield of

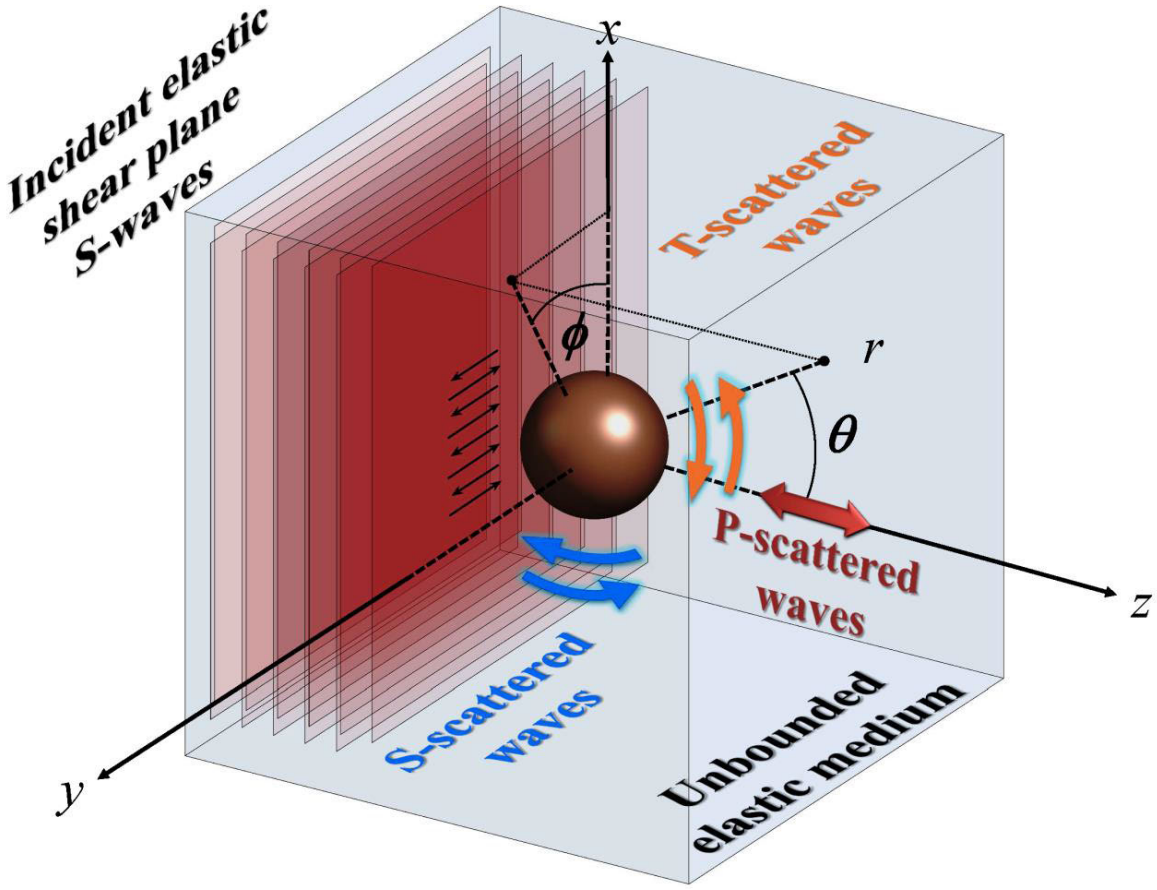

FIGURE 1. Geometry of the problem. An incident elastic plane wave field composed of linearly-polarized shear plane progressive waves, and characterized by its vector potential (described by the arrows) is incident upon an elastic sphere embedded in an infinite elastic matrix. The direction of wave propagation is along the longitudinal *z*-axis.

continuous elastic waves to the embedded sphere, a mean (time-averaged) radiation force arises, which constitutes the subject of the present study.

In this investigation, the mean elastic force exerted on a solid sphere, encased in a homogeneous linearly-elastic unbounded medium, is derived based on the integration of the radial component of the elastodynamic Poynting vector (known also as the power flow density vector) over a virtual spherical surface of large radius R enclosing the particle. Initially, the elastic scattering of shear plane progressive waves by a solid sphere is determined. The modal expansion method in spherical coordinates [31] and adequate boundary matching are used to compute the scattering coefficients [29], [30]. Then, integration of the power flow density vector component and algebraic manipulation lead to the exact mathematical expression for the mean force. Particular attention is paid to elastic mode preservation and conversion in the framework of linear elasticity. A quantitative verification and validation of the method (applicable only for progressive waves) is also accomplished based on the expressions of the extinction efficiency and the scattering asymmetry parameter. Note that the method based on the elastodynamic Poynting vector formalism is general and applicable to other wavefronts of arbitrary shape, and will be presented in forthcoming works. Computations for the dimensionless mean radiation force efficiency and its components related to mode preservation and conversion provide useful information and fundamental physical understanding of the theoretical analysis. Moreover, it is important to note that the derived equations for the radiation force efficiency are exact, not restricted to a particular range of frequencies, and obtained without any approximations.

II. ELASTIC WAVE SCATTERING BY A SPHERE

A wave-field, composed of plane progressive shear waves, with its incident vector displacement *potential* polarized along the y-axis (with $\mathbf{e}_y$ being the unit vector along the y-axis) propagates along the z-axis of a system of coordinates centered on a solid sphere (Fig. 1). Notice that the incident particle *displacement vector* is polarized along the x-axis. The medium of wave propagation is assumed to be linearly-elastic, homogeneous, lossless and isotropic. The incident elastic shear plane progressive wave-field is expressed by a vector displacement potential as [29],

$$\begin{aligned}\boldsymbol{\Psi}^{S}_{inc,pr} &= \psi_0 \mathrm{e}^{i(k_S z-\omega t)}\mathbf{e}_y \\ &= \boldsymbol{\nabla}\times\left(\mathbf{r}\psi^{S}_{inc,pr}\right)+\boldsymbol{\nabla}\times\left[\boldsymbol{\nabla}\times\left(\mathbf{r}\chi^{T}_{inc,pr}\right)\right], \quad (1)\end{aligned}$$

where ψ_0 is the displacement potential amplitude, $k_S = \omega/c_S$ is the wavenumber of the shear wave-field in the elastic lossless matrix, ω is the angular frequency, c_S is the speed of sound for the shear propagating waves, $\mathbf{r}$ is the position vector, and $\psi^S_{inc,pr}$ and $\chi^T_{inc,pr}$ are the two scalar (Debye) potentials describing the incident shear wave-field with a linear polarization state established *a priori*.

Using spherical wave functions, the scalar potentials in Eq.(1) are expressed by means of partial-wave series expansions as [29],

$$\begin{pmatrix} \psi^S_{inc,pr} \\ \chi^T_{inc,pr} \end{pmatrix} = -\psi_0 e^{-i\omega t} \sum_{n=1}^{+\infty} i^n \frac{(2n+1)}{n(n+1)} j_n(k_S r) \times P_n^1(\cos\theta) \begin{pmatrix} \cos\phi \\ (i/k_S)\sin\phi \end{pmatrix}, \tag{2}$$

where $j_n(\cdot)$ is the spherical Bessel function of the first kind and $P_n^1(\cdot)$ are the associated Legendre functions of the first order, and θ and ϕ are the polar and azimuthal angles, respectively.

The solid sphere is perfectly bonded to the elastic matrix in which the scattered elastic waves propagate. As discussed previously in Section I, and shown explicitly in [29] and [30], the scattered propagating fields are related to *mode-converted* waves S → P, while the remaining ones are mode-preserved S → S and T → T scattered waves. Their associated displacement potential functions are expressed using three scalar potentials as [29],

$$\begin{pmatrix} \Phi^{S\to P}_{sca,pr} \\ \psi^{S\to S}_{sca,pr} \\ \chi^{T\to T}_{sca,pr} \end{pmatrix} = -\psi_0 e^{-i\omega t} \sum_{n=1}^{+\infty} i^n \frac{(2n+1)}{n(n+1)} P_n^1(\cos\theta) \times \begin{pmatrix} S_n^{S\to P} h_n^{(1)}(k_P r)\cos\phi \\ S_n^{S\to S} h_n^{(1)}(k_S r)\cos\phi \\ S_n^{T\to T}(i/k_S) h_n^{(1)}(k_S r)\sin\phi \end{pmatrix}, \tag{3}$$

where $h_n^{(1)}(\cdot)$ is the spherical Hankel function of the first kind of order n, k_P $(= \omega/c_P)$ is the wavenumber of the compressional wave in the elastic lossless matrix and c_P is the speed of sound of the compressional wave. $S_n^{S\to P}$ is the scattering coefficient for the waves resulting from shear-to-compressional mode conversion, while $S_n^{S\to S}$ and $S_n^{T\to T}$ correspond to shear-to-shear and transverse-to-transverse mode preservation.

The elastic waves transmitted inside the embedded elastic sphere are described by the potentials [29]

$$\begin{pmatrix} \Phi^{S\to P}_{int,pr} \\ \psi^{S\to S}_{int,pr} \\ \chi^{T\to T}_{int,pr} \end{pmatrix} = -\psi_0 e^{-i\omega t} \sum_{n=1}^{+\infty} i^n \frac{(2n+1)}{n(n+1)} P_n^1(\cos\theta) \times \begin{pmatrix} S^{S\to P}_{int,n} j_n(k_{int,P} r)\cos\phi \\ S^{S\to S}_{int,n} j_n(k_{int,S} r)\cos\phi \\ S^{T\to T}_{int,n}(i/k_{int,S}) j_n(k_{int,S} r)\sin\phi \end{pmatrix}, \tag{4}$$

where the scattering coefficients $S^{S\to\{P,S\}}_{int,n}$, $S^{T\to T}_{int,n}$, and the wavenumbers $k_{int,\{P,S\}} = \omega/c_{int,\{P,S\}}$ are for the compressional, shear and transverse waves propagating in the sphere material, respectively.

The continuity of the displacement and stress components at the interface lead to a linear system of equations written as [30],

$$\begin{bmatrix} d_{11} & d_{12} & d_{13} & d_{14} \\ d_{21} & d_{22} & d_{23} & d_{24} \\ d_{31} & d_{32} & d_{33} & d_{34} \\ d_{41} & d_{42} & d_{43} & d_{44} \end{bmatrix} \begin{Bmatrix} S_n^{S\to P} \\ S_n^{S\to S} \\ S^{S\to P}_{int,n} \\ S^{S\to S}_{int,n} \end{Bmatrix} = -\Re \begin{Bmatrix} d_{12} \\ d_{22} \\ d_{32} \\ d_{42} \end{Bmatrix}$$

$$\begin{bmatrix} d_{55} & d_{56} \\ d_{65} & d_{66} \end{bmatrix} \begin{Bmatrix} S_n^{T\to T} \\ S^{T\to T}_{int,n} \end{Bmatrix} = -\Re \begin{Bmatrix} d_{55} \\ d_{65} \end{Bmatrix}, \tag{5}$$

where the matrix elements d_{ij} are listed explicitly in Appendix B of [30], and $\Re\{\cdots\}$ denotes the real part of a complex number.

III. MEAN ELASTIC LONGITUDINAL RADIATION FORCE

Adequate derivation of the mean (time-averaged) elastic radiation force on a particle in an elastic medium is accomplished using the integration of the radial component of the elastodynamic Poynting vector over a virtual surface enclosing the object. This procedure was applied successfully for the case of a cylindrical inclusion [32], [33]. Stemming from the expressions of the incident and scattered scalar potentials given in Section II, the mean elastic force of shear waves is obtained as,

$$\overline{\mathbf{F}^S} = -\frac{1}{c_S} \iint_{\Gamma} \left(\overline{\prod^S_{tot}} \cdot \mathbf{e}_r \right) d\mathbf{\Gamma}, \tag{6}$$

where the overbar symbol $\overline{\cdots}$ denotes time-averaging over a cycle of the harmonic wave, $\overline{\prod^S_{tot}} = -\frac{1}{2}\Re\left\{ i\omega\, \mathbf{u}^{S*}_{tot} \cdot \overleftrightarrow{\boldsymbol{\tau}}^S_{tot} \right\}$, is the mean total (incident + scattered) power flow density vector [34], [35] (which is the elastodynamic counterpart of the Poynting vector in electromagnetic theory), $\mathbf{u}^S_{tot}$ and $\overleftrightarrow{\boldsymbol{\tau}}^S_{tot}$ are the total (incident + scattered) displacement vector and elastic stress tensor, respectively, the superscript $*$ is the complex conjugate, $\mathbf{e}_r$ is the radial unit vector, $d\mathbf{\Gamma}$ is the differential spherical surface vector and Γ is a spherical surface of large radius $R \gg a$ enclosing the sphere of radius a.

Because the incident plane shear wave-field is propagating along the z-direction, only the longitudinal component of the mean elastic is obtained. A longitudinal *dimensionless* radiation force efficiency (or function) for shear (S) elastic plane progressive waves is defined as,

$$Y^S_{pr} = \frac{\overline{\mathbf{F}^S} \cdot \mathbf{e}_z}{(\pi a^2) E^S_0} = \frac{1}{(\pi k_S a^2 \rho \omega^3 |\psi_0|^2)}$$

$$\times \int_0^{2\pi}\int_0^{\pi}\Big[\Re\Big\{i\omega\Big(u^{S*}_{tot,r}\tau^{S}_{tot,rr}+u^{S*}_{tot,\theta}\tau^{S}_{tot,r\theta} +u^{S*}_{tot,\phi}\tau^{S}_{tot,r\phi}\Big)\Big\} \times R^2\sin\theta\cos\theta\,d\theta\,d\phi\Big], \tag{7}$$

where $E_0^S = \frac{1}{2c_S}\rho k_S\omega^3|\psi_0|^2$ is a characteristic energy density factor, and $\mathbf{e}_z$ is the longitudinal unit vector along the z-axis. The parameter ρ is the mass density of the elastic matrix, and $u^S_{tot,r}$, $u^S_{tot,\theta}, u^S_{tot,\phi}$, $\tau^S_{tot,rr}, \tau^S_{tot,r\theta}$, and $\tau^S_{tot,r\phi}$ are the radial, polar and azimuthal components of the *total* (incident + scattered) displacement vector and elastic stress tensor, respectively, given in Appendix A of [30]. Notice that the double integral in Eq.(7), with terms involving products of the incident field, i.e., $\left(u^{S*}_{inc,r}\tau^S_{inc,rr}+u^{S*}_{inc,\theta}\tau^S_{inc,r\theta}+u^{S*}_{inc,\phi}\tau^S_{inc,r\phi}\right)$ vanish, as there is no mean force if the sphere is absent.

The substitution of the potentials into the expressions of the displacement vector and stress tensor components into Eq.(7) leads after some algebraic manipulation to the exact partial-wave series expansion for elastic shear plane progressive waves as,

$$\begin{aligned}Y^S_{pr} = &-\frac{2}{(k_Sa)^2}\\ &\times\sum_{n=1}^{+\infty}\frac{1}{(n+1)}\Big\{n\,(n+2)\Big[\alpha_n^{S\to S}+\alpha_{n+1}^{S\to S}+\alpha_n^{T\to T}+\alpha_{n+1}^{T\to T}\\ &+2\left(\alpha_n^{S\to S}\alpha_{n+1}^{S\to S}+\beta_n^{S\to S}\beta_{n+1}^{S\to S}+\alpha_n^{T\to T}\alpha_{n+1}^{T\to T}\right.\\ &\left.+\beta_n^{T\to T}\beta_{n+1}^{T\to T}\right)\Big]\\ &+\frac{(2n+1)}{n}\Big[\alpha_n^{S\to S}+\alpha_n^{T\to T}\\ &+2\left(\alpha_n^{S\to S}\alpha_n^{T\to T}+\beta_n^{S\to S}\beta_n^{T\to T}\right)\Big]\\ &+2\left(\frac{c_P}{c_S}\right)\left(\alpha_n^{S\to P}\alpha_{n+1}^{S\to P}+\beta_n^{S\to P}\beta_{n+1}^{S\to P}\right)\Big\},\end{aligned} \tag{8}$$

where $\alpha_n^{\{S\to P,S\to S,T\to T\}} = \Re\left\{S_n^{\{S\to P,S\to S,T\to T\}}\right\}$, $\beta_n^{\{S\to P,S\to S,T\to T\}} = \Im\left\{S_n^{\{S\to P,S\to S,T\to T\}}\right\}$, respectively, and $\Im\{\cdots\}$ is the imaginary part of a complex number.

To further highlight the different contributions, Eq.(8) is decomposed into the sum of four individual components as,

$$Y^S_{pr} = Y^{(S\to S)}_{pr} + Y^{(T\to T)}_{pr} + Y^{(S\to S,T\to T)}_{pr} + Y^{(S\to P)}_{pr}. \tag{9}$$

The components $Y^{(S\to S)}_{pr}$ and $Y^{(T\to T)}_{pr}$ related to *mode preservation* are given, respectively, as,

$$\begin{aligned}Y^{(S\to S)}_{pr} = &-\frac{2}{(k_Sa)^2}\sum_{n=1}^{+\infty}\frac{1}{(n+1)}\Big\{n\,(n+2)\Big[\alpha_n^{S\to S}+\alpha_{n+1}^{S\to S}\\ &+2\left(\alpha_n^{S\to S}\alpha_{n+1}^{S\to S}+\beta_n^{S\to S}\beta_{n+1}^{S\to S}\right)\Big]\\ &+\frac{(2n+1)}{n}\alpha_n^{S\to S}\Big\},\end{aligned} \tag{10}$$

$$\begin{aligned}Y^{(T\to T)}_{pr} = &-\frac{2}{(k_Sa)^2}\sum_{n=1}^{+\infty}\frac{1}{(n+1)}\Big\{n\,(n+2)\Big[\alpha_n^{T\to T}+\alpha_{n+1}^{T\to T}\\ &+2\left(\alpha_n^{T\to T}\alpha_{n+1}^{T\to T}+\beta_n^{T\to T}\beta_{n+1}^{T\to T}\right)\Big]\\ &+\frac{(2n+1)}{n}\alpha_n^{T\to T}\Big\}.\end{aligned} \tag{11}$$

The component $Y^{(S\to S,T\to T)}_{pr}$, which is related to *shear and transverse mode coupling*, is expressed as,

$$\begin{aligned}Y^{(S\to S,T\to T)}_{pr} = &-\frac{4}{(k_Sa)^2}\\ &\times\sum_{n=1}^{+\infty}\frac{(2n+1)}{n\,(n+1)}\\ &\times\left(\alpha_n^{S\to S}\alpha_n^{T\to T}+\beta_n^{S\to S}\beta_n^{T\to T}\right).\end{aligned} \tag{12}$$

Finally, the component $Y^{(S\to P)}_{pr}$ related to *shear-to-compression mode conversion* is given as,

$$\begin{aligned}Y^{(S\to P)}_{pr} = &-\frac{4}{(k_Sa)^2}\left(\frac{c_P}{c_S}\right)\\ &\times\sum_{n=1}^{+\infty}\frac{1}{(n+1)}\left(\alpha_n^{S\to P}\alpha_{n+1}^{S\to P}+\beta_n^{S\to P}\beta_{n+1}^{S\to P}\right).\end{aligned} \tag{13}$$

From a mathematical analysis, Eq.(13) shows a dependence on the factor $1/(n+1)$ that approaches zero as n increases. This dependence will predict the behavior of a negligible mode conversion as will be shown subsequently.

The decomposition of Eq.(8) as written by Eq.(9) reveals important information regarding the factors that contribute to the mean elastic force of shear plane progressive waves. One notices some regularity in the expressions given by Eqs.(10) and (11). Those components are related to pure shear and transverse mode preservation and contribute directly to the total force efficiency. Interestingly, Eq.(12) shows that shear and transverse mode coupling occurs, and contributes separately to the mean elastic force efficiency. Although the linear elastic resonance scattering theory involving shear elastic plane progressive waves [29] does not predict a coupling of shear and transverse waves, it is however manifested in the mean elastic radiation force because it is a *quadratic* (second-order) observable. On the other hand, the shear and transverse wave coupling was not manifested in the formalism of the mean elastic force of incident shear elastic plane progressive waves for a cylinder embedded in a solid at normal incidence [32], [33] (obtained in 2D). Lastly, Eq.(13) shows the contribution of mode conversion to the elastic radiation force efficiency.

IV. VERIFICATION AND VALIDATION BASED UPON THE EXTINCTION ENERGY EFFICIENCY, AND SCATTERING ASYMMETRY PARAMETER

A different method to evaluate the elastic force of plane shear waves on a lossless particle can be employed, which is based

on the expressions of the extinction (or scattering) energy efficiency and the scattering asymmetry parameter. This method was presented in seminal works in acoustics [36], [37], [38] for a sphere (and a cylinder; see Eq.(18) in [39]) submerged in a non-viscous fluid, and later extended for an elastic medium [40]. In essence, the dimensionless longitudinal mean force efficiency for elastic shear plane progressive waves can be expressed as,

$$Y_{pr}^{S} = Q_{ext}^{S} - Q_{sca}^{S} \langle \cos\theta \rangle , \tag{14}$$

where Q_{ext}^{S} is a dimensionless observable corresponding to the extinction energy efficiency. This quadratic quantity is the sum of the scattering and absorption energy efficiencies, and $Q_{sca}^{S} \langle \cos\theta \rangle$ is the dimensionless scattering asymmetry parameter, where the symbol $\langle \cdots \rangle$ denotes spatial averaging (along the longitudinal direction, i.e. $\langle \cos\theta \rangle$).

The dimensionless extinction energy efficiency for a sphere embedded in an elastic solid medium is determined as [34], [35],

$$\begin{aligned} Q_{ext}^{S} &= -\frac{1}{(\pi a^2)\, W_0^S} \iint_{\Gamma} \left(\overline{\prod_{is}^{S}} \cdot \mathbf{e}_r \right) d\Gamma \\ &= -\frac{2}{(k_S a)^2} \sum_{n=1}^{+\infty} (2n+1) \left[\alpha_n^{S\to S} + \alpha_n^{T\to T} \right], \end{aligned} \tag{15}$$

where $\overline{\prod_{is}^{S}} = -\frac{1}{2}\Re\left\{ i\omega \left(\mathbf{u}_{inc}^{S*} \cdot \overleftrightarrow{\boldsymbol{\tau}}_{sca}^{S} + \mathbf{u}_{sca}^{S*} \cdot \overleftrightarrow{\boldsymbol{\tau}}_{inc}^{S} \right) \right\}$, and $W_0^S = \frac{1}{2}\rho\omega^3 k_S |\psi_0|^2$ is a characteristic power coefficient.

In a similar approach, the scattering asymmetry parameter is calculated based upon the expression of the scattering energy efficiency [34], [35], for which the integral expression is given by,

$$Q_{sca}^{S} \langle \cos\theta \rangle = \frac{1}{(\pi a^2)\, W_0^S} \iint_{\Gamma} \left(\overline{\prod_{sca}^{S}} \cdot \mathbf{e}_r \right) \cos\theta \, d\Gamma, \tag{16}$$

where $\overline{\prod_{sca}^{S}} = -\frac{1}{2}\Re\left\{ i\omega\, \mathbf{u}_{sca}^{S*} \cdot \overleftrightarrow{\boldsymbol{\tau}}_{sca}^{S} \right\}$.

Upon the substitution of the displacement and stress tensor components into Eq.(16) using the expressions of the potentials, a partial-wave series expression for the dimensionless scattering asymmetry parameter is obtained as,

$$\begin{aligned} &Q_{sca}^{S} \langle \cos\theta \rangle \\ &= \frac{4}{(k_S a)^2} \sum_{n=1}^{+\infty} \frac{1}{(n+1)} \left\{ n(n+2) \left[\alpha_n^{S\to S} \alpha_{n+1}^{S\to S} \right.\right. \\ &\quad \left. + \beta_n^{S\to S} \beta_{n+1}^{S\to S} + \alpha_n^{T\to T} \alpha_{n+1}^{T\to T} + \beta_n^{T\to T} \beta_{n+1}^{T\to T} \right] \\ &\quad + \frac{(2n+1)}{n} \left[\alpha_n^{S\to S} \alpha_n^{T\to T} + \beta_n^{S\to S} \beta_n^{T\to T} \right] \\ &\quad \left. + \left(\frac{c_P}{c_S} \right) \left[\alpha_n^{S\to P} \alpha_{n+1}^{S\to P} + \beta_n^{S\to P} \beta_{n+1}^{S\to P} \right] \right\}, \end{aligned} \tag{17}$$

Similarly to Eq.(9), $Q_{sca}^{S} \langle \cos\theta \rangle$ is expressed as the sum of four components as,

$$\begin{aligned} Q_{sca}^{S} \langle \cos\theta \rangle &= Q_{sca}^{(S\to S)} \langle \cos\theta \rangle + Q_{sca}^{(T\to T)} \langle \cos\theta \rangle \\ &\quad + Q_{sca}^{(S\to S, T\to T)} \langle \cos\theta \rangle + Q_{sca}^{(S\to P)} \langle \cos\theta \rangle , \end{aligned} \tag{18}$$

where the mode preservation components are given as,

$$\begin{aligned} Q_{sca}^{(S\to S)} \langle \cos\theta \rangle &= \frac{4}{(k_S a)^2} \\ &\quad \times \sum_{n=1}^{+\infty} \frac{n(n+2)}{(n+1)} \\ &\quad \times \left[\alpha_n^{S\to S} \alpha_{n+1}^{S\to S} + \beta_n^{S\to S} \beta_{n+1}^{S\to S} \right], \end{aligned} \tag{19}$$

$$\begin{aligned} Q_{sca}^{(T\to T)} \langle \cos\theta \rangle &= \frac{4}{(k_S a)^2} \\ &\quad \times \sum_{n=1}^{+\infty} \frac{n(n+2)}{(n+1)} \\ &\quad \times \left[\alpha_n^{T\to T} \alpha_{n+1}^{T\to T} + \beta_n^{T\to T} \beta_{n+1}^{T\to T} \right]. \end{aligned} \tag{20}$$

The component related to shear and transverse mode coupling is expressed as,

$$\begin{aligned} Q_{sca}^{(S\to S, T\to T)} \langle \cos\theta \rangle &= \frac{4}{(k_S a)^2} \\ &\quad \times \sum_{n=1}^{+\infty} \frac{(2n+1)}{n(n+1)} \\ &\quad \times \left[\alpha_n^{S\to S} \alpha_n^{T\to T} + \beta_n^{S\to S} \beta_n^{T\to T} \right], \end{aligned} \tag{21}$$

and the contribution from mode conversion to the scattering asymmetry parameter is expressed as,

$$\begin{aligned} Q_{sca}^{(S\to P)} \langle \cos\theta \rangle &= \frac{4}{(k_S a)^2} \left(\frac{c_P}{c_S} \right) \\ &\quad \times \sum_{n=1}^{+\infty} \frac{1}{(n+1)} \\ &\quad \times \left[\alpha_n^{S\to P} \alpha_{n+1}^{S\to P} + \beta_n^{S\to P} \beta_{n+1}^{S\to P} \right]. \end{aligned} \tag{22}$$

The substitution of Eq.(15) and (17) into Eq.(14) leads to the expression of the dimensionless longitudinal elastic radiation force efficiency as,

$$\begin{aligned} Y_{pr}^{S} &= -\frac{2}{(k_S a)^2} \sum_{n=1}^{+\infty} (2n+1) \left[\alpha_n^{S\to S} + \alpha_n^{T\to T} \right] \\ &\quad + \frac{2}{(n+1)} \left\{ n(n+2) \left[\alpha_n^{S\to S} \alpha_{n+1}^{S\to S} + \beta_n^{S\to S} \beta_{n+1}^{S\to S} \right.\right. \\ &\quad \left. + \alpha_n^{T\to T} \alpha_{n+1}^{T\to T} + \beta_n^{T\to T} \beta_{n+1}^{T\to T} \right] \\ &\quad + \frac{(2n+1)}{n} \left[\alpha_n^{S\to S} \alpha_n^{T\to T} + \beta_n^{S\to S} \beta_n^{T\to T} \right] \\ &\quad \left. + \left(\frac{c_P}{c_S} \right) \left[\alpha_n^{S\to P} \alpha_{n+1}^{S\to P} + \beta_n^{S\to P} \beta_{n+1}^{S\to P} \right] \right\}, \end{aligned} \tag{23}$$

which is apparently different from the expression given by Eq.(8) using the integration of the elastodynamic Poynting

vector in the far-field. Comparison of the two expressions, and further algebraic analysis and mathematical manipulation demonstrate that,

$$\begin{aligned}
&\sum_{n=1}^{+\infty}\frac{1}{(n+1)}\left\{n\,(n+2)\left[\alpha_n^{S\to S}+\alpha_{n+1}^{S\to S}+\alpha_n^{T\to T}+\alpha_{n+1}^{T\to T}\right]\right.\\
&\quad\left.+\frac{(2n+1)}{n}\left[\alpha_n^{S\to S}+\alpha_n^{T\to T}\right]\right\}\\
&=\frac{1}{2}\begin{pmatrix}3\alpha_1^{S\to S}+3\alpha_2^{S\to S}\\+3\alpha_1^{T\to T}+3\alpha_2^{T\to T}\end{pmatrix}\\
&\quad+\frac{3}{2}\left(\alpha_1^{S\to S}+\alpha_1^{T\to T}\right)\\
&\quad+\frac{1}{3}\begin{pmatrix}8\alpha_2^{S\to S}+8\alpha_3^{S\to S}\\+8\alpha_2^{T\to T}+8\alpha_3^{T\to T}\end{pmatrix}\\
&\quad+\frac{5}{6}\left(\alpha_2^{S\to S}+\alpha_2^{T\to T}\right)+\ldots\\
&=3\alpha_1^{S\to S}+3\alpha_1^{T\to T}+5\alpha_2^{S\to S}+5\alpha_2^{T\to T}+7\alpha_3^{S\to S}\\
&\quad+7\alpha_3^{T\to T}+\ldots\\
&=\sum_{n=1}^{+\infty}(2n+1)\left[\alpha_n^{S\to S}+\alpha_n^{T\to T}\right].
\end{aligned}\tag{24}$$

It has been also verified that the series are equivalent when the coefficients α_n are replaced by β_n in Eq.(24). Hence, the equality is also valid for the scattering coefficients and can be written as,

$$\begin{aligned}
&\sum_{n=1}^{+\infty}\frac{1}{(n+1)}\left\{n\,(n+2)\left[S_n^{S\to S}+S_{n+1}^{S\to S}+S_n^{T\to T}+S_{n+1}^{T\to T}\right]\right.\\
&\quad\left.+\frac{(2n+1)}{n}\left[S_n^{S\to S}+S_n^{T\to T}\right]\right\}\\
&=\sum_{n=1}^{+\infty}(2n+1)\left[S_n^{S\to S}+S_n^{T\to T}\right].
\end{aligned}\tag{25}$$

Keeping the equality given by Eq.(24) in mind, adequate substitution into Eq.(23) and algebraic manipulation shows that the series are equal and commensurate with the same result.

V. ASYMMETRY PARAMETER

The asymmetry parameter $\langle\cos\theta\rangle$ is a factor that provides quantitative information about the directivity of the scattered energy. If $\langle\cos\theta\rangle \to 1$, the scattered energy from the sphere is directed along the direction of wave propagation. However, if $\langle\cos\theta\rangle \to -1$, the scattered energy is direct along the opposite direction of wave propagation.

Because the solid lossless sphere is embedded in an elastic medium with no attenuation, the absorption energy efficiency, $Q_{abs}^S = \left(Q_{ext}^S - Q_{sca}^S\right) = 0$. Consequently, Eq.(14) is rewritten in terms of the scattering energy efficiency as,

$$Y_{pr}^S = Q_{sca}^S\left(1-\langle\cos\theta\rangle\right), \tag{26}$$

where [34], [35],

$$\begin{aligned}
Q_{sca}^S &= \frac{1}{(\pi a^2)\,W_0^S}\iint_{\Gamma}\left(\overline{\prod_{sca}^S}\cdot\,\mathbf{e}_r\right)d\Gamma\\
&=\frac{2}{(k_S a)^2}\sum_{n=1}^{+\infty}(2n+1)\\
&\quad\times\begin{bmatrix}\alpha_n^{S\to S^2}+\beta_n^{S\to S^2}+\alpha_n^{T\to T^2}+\beta_n^{T\to T^2}\\+\frac{1}{n(n+1)}\left(\frac{c_P}{c_S}\right)\left(\alpha_n^{S\to P^2}+\beta_n^{S\to P^2}\right)\end{bmatrix}.
\end{aligned}\tag{27}$$

Using Eq.(17) and (27), the mathematical expression of the asymmetry parameter $\langle\cos\theta\rangle$ assuming shear plane elastic waves can be obtained as the ratio of two partial-wave series expansions. Also, it is noticed from Eq.(27) that the individual contributions to the scattering energy efficiency originate from mode preservation S → S and T → T, as well as mode conversion S → P. By inspecting the component related to mode conversion S → P, it is anticipated that its contribution is minimal because of the factor $1/[n\,(n+1)]$ that decays substantially as the integer n increases. Furthermore, Eq.(27) shows that there is no coupling between the shear and transverse waves, in contrast to what has been established for the total mean force efficiency Y_{pr}^S and the scattering asymmetry parameter $Q_{sca}\,\langle\cos\theta\rangle$.

VI. NUMERICAL RESULTS AND DISCUSSIONS

The theory is now illustrated by performing numerical computations of Eq.(8), which is the main contribution of this work. Furthermore, the individual components of the mean radiation force efficiency are evaluated as well to provide an improved interpretation of the results.

First, a solid sphere implanted in a soft elastic gel matrix with perfect bonding is considered. The physical parameters of the materials are the mass densities of the sphere chosen as brass (chosen as an example), $\rho_{int} = 8100\,kg/m^3$ and the elastic host medium, $\rho = 1100\,kg/m^3$, where the compressional and shear sound speeds are given, respectively, as $c_{int,P} = 3830\,m/s$, $c_{int,S} = 2050\,m/s$, $c_P = 1550\,m/s$, and $c_S = 100\,m/s$ [41]. Truncation of the series was done at a maximum limit largely exceeding $k_S a$ to ensure convergence, such that $N_{\max} = \text{round}[k_S a + 4.05\sqrt[3]{k_S a} + 5]$. The choice of the maximum truncation limit was obtained by increasing the partial-wave index n while computing the relative numerical error (in the order of $\sim 10^{-12}$) and checking the stability of the curves.

The corresponding results for the mean elastic force efficiency and its components are shown in the plots of Fig. 2. Clearly, one large resonance peak arises in the plot of the longitudinal radiation force function Y_{pr}^S near $k_S a \approx 0.85$, which mainly corresponds to a dipole (n= 1) mode vibration of the sphere. This corresponds to a rigid-body translational motion of the sphere within the gel matrix, despite the fact that the elastic scattering is transversal for $n = 1$. By analyzing the elastic shear and transverse Debye potentials, it is evident from Eq.(3) the dependence on the associated Legendre functions of the first order. For n= 1, $P_1^1(\cos\theta) = 0$ for $\theta = 0$

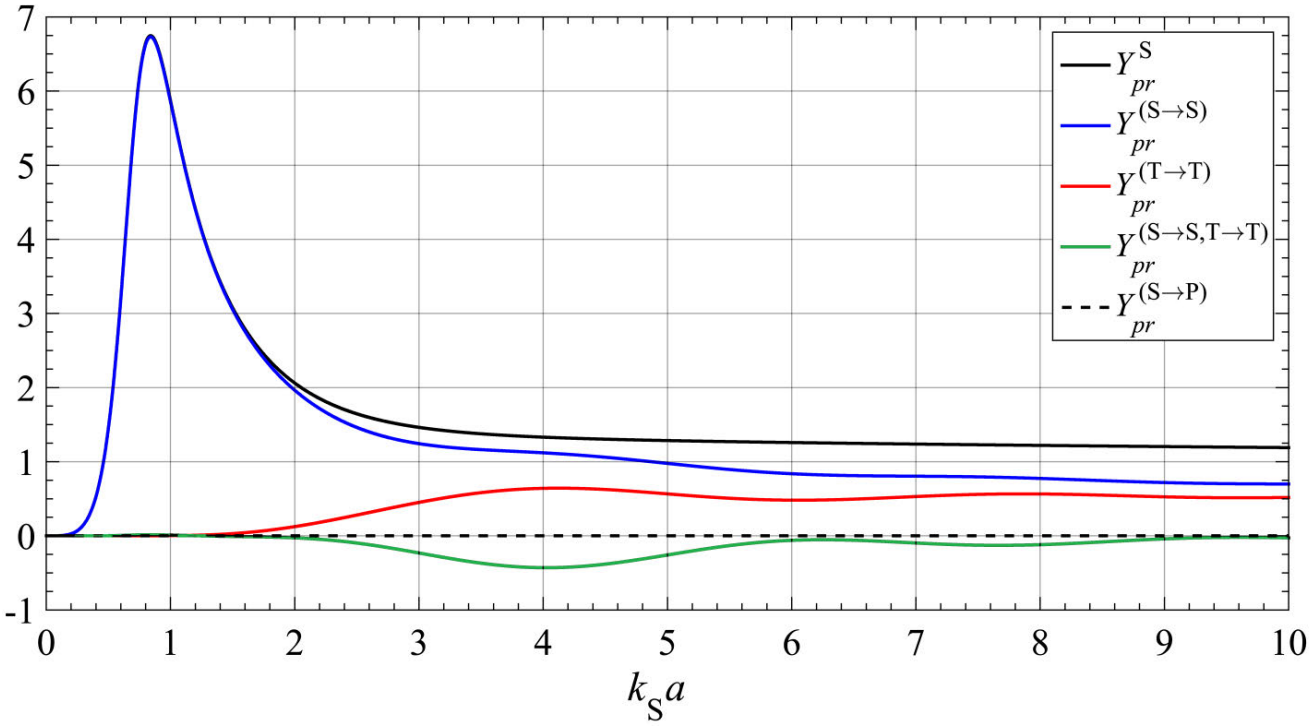

FIGURE 2. The plots for the mean elastic radiation force efficiency and its individual components, assuming shear (S) elastic plane progressive waves incident upon an elastic brass sphere in a soft gel matrix.

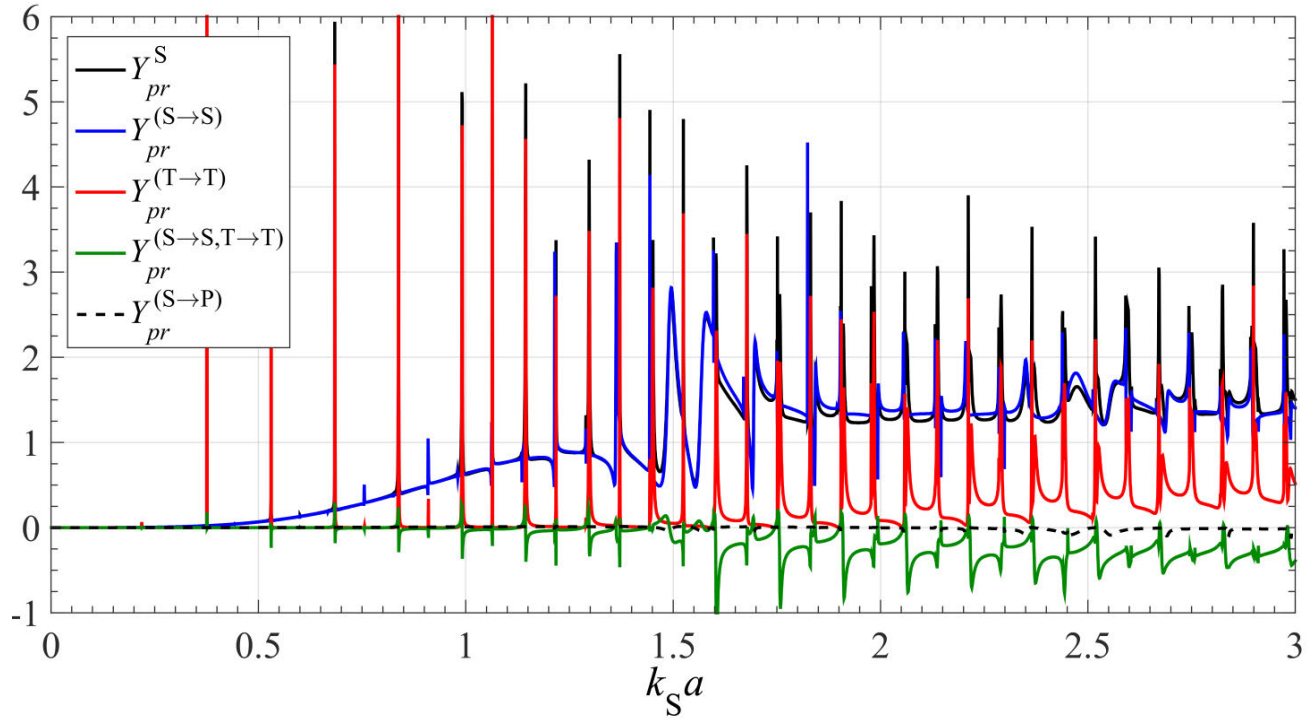

FIGURE 3. The plots for the mean elastic radiation force efficiency and its individual components, assuming shear (S) elastic plane progressive waves incident upon an elastic soft gel sphere embedded in a brass elastic matrix.

or $\theta = \pi$. As such, the elastic dipole scattering is purely transversal in the (xy)-plane, with maxima along the directions $\theta = \pm\,\pi/2$ and $\phi = 0$ or π for S→S scattering, and $\phi = \pm\,\pi/2$ for T→T scattering, respectively. However, other modes of different amplitudes contribute to the total elastic scattering field. Notice that Y_{pr}^{S} is always positive, suggest-

ing that the mean force always acts along the longitudinal z-direction of elastic wave motion. In the bandwidth $k_S a < 2$, it is shown that the shear-to-shear (S → S) mode preservation dominates such that $Y_{pr}^{S} \approx Y_{pr}^{(S\to S)}$. As $k_S a$ increases beyond this value, the positive contribution of $Y_{pr}^{(T\to T)}$ to the total force efficiency becomes more prominent, while the component related to the coupling $Y_{pr}^{(S\to S,T\to T)}$ contributes negatively. The plot for $Y_{pr}^{(S\to P)} \approx 0$, regardless of the value of $k_S a$, suggesting that the mode conversion component has a negligible effect on the total mean force, and hence, can be ignored.

Additional calculations are performed now for the contrasting case of a soft gel sphere encased in a brass elastic matrix. The dimensionless size parameter was varied in the range $0 < k_S a \leq 3$ and the results are displayed in Fig. 3. In contrast with the plots in Fig. 2, a series of sharp resonance maxima and minima peaks are excited, except for the mode conversion component, with its amplitude oscillating around zero. Again for this case, the contribution of $Y_{pr}^{(S\to P)}$ to the total efficiency Y_{pr}^{S} is negligible. The shear-to-shear component $Y_{pr}^{(S\to S)}$ is always positive, whereas $Y_{pr}^{(T\to T)}$ can take negative values between two consecutive resonance peaks. Furthermore, the coupling factor $Y_{pr}^{(S\to S,T\to T)}$ is mainly negative, while it can reverses it sign at some of the resonances. In essence, the change in the physical/mechanical properties of the elastic matrix alters the contributions of the sear-to-shear and transverse-to-transverse mode preservations and their coupling, while the mode conversion contribution $Y_{pr}^{(S\to P)}$ to the total force function Y_{pr}^{P} is negligible.

VII. CONCLUSION

In this analysis, the time-averaged elastic radiation force induced by shear, linearly-polarized plane progressive waves on a solid sphere, embedded in an elastic medium is investigated, in contrast with the case of compressional elastic waves [42]. A theoretical analysis stemming from the elastic shear-wave scattering is developed and exact partial-wave series expressions are provided without any approximations. The analysis is based on integrating the time-averaged radial component of the power flow density vector (or the elastodynamic Poynting vector) to obtain the longitudinal component of the mean force. Separation of the total force efficiency into individual components shows the distinct contributions of shear-to-shear, transverse-to-transverse mode preservation as well as their coupling, in addition to mode conversion. Adequate verification and validation based on the expression of the extinction and scattering efficiencies in conjunction with the asymmetry parameter leads to an equivalent solution for the mean elastic force efficiency. Numerical simulations and computational results for the dimensionless radiation force efficiency and its individual components show the significance of the contribution of each component to the total force efficiency. In essence, for the examples chosen here for a stiff solid sphere in a soft elastic matrix, or a soft sphere in a stiff elastic matrix, the contribution of mode conversion S → P can be considered negligible. This effect is explained by mathematical analysis of the partial-wave series expansion of the scattering energy efficiency, and the component related to mode conversion which decreases significantly as the partial-wave number $n$increases. For a stiff sphere in a soft matrix, the component related to S → S mode preservation dominates and contributes the most to the total mean force efficiency for $k_S a < 2$. In contrast with the case of compressional waves [42], the dimensionless radiation force function is larger for shear progressive waves. For a soft sphere in a stiff elastic matric, both S → S and T → T mode preservation and their coupling contribute individually to the mean force, especially at the resonances. The component related to the coupling between S → S and T → T waves is mainly negative, suggesting a weakening of the total efficiency. In other words, the component related to the S → S and T → T coupling has the tendency to create generally a pulling negative force component; however, the total mean force efficiency remains positive. Notice that metamaterials may have the ability to suppress mode conversion [43], and potential modification of the present formalism can be applied to investigate the mean elastic force for such unconventional media. The present theory and analytical formalism may find some applications in elastography and elasticity imaging applications, activation/triggering of implantable devices [44], [45], [46], [47], [48] using shear-waves, and possibly other areas in soft matter and condensed matter physics. It must be also noted that mode preservation, coupling, and conversion can be found in electromagnetic theory, especially in materials exhibiting rotary polarization (known also as circular dichroism) as shown in related works in electromagnetic/optical scattering, radiation force, and torque [49], [50], [51], [52].

ACKNOWLEDGMENT

The views, analyses, methods, results, discussions, findings, and conclusions expressed in this manuscript belong solely and exclusively to the author, and do not reflect the opinions, policies, or position of Schlumberger, SLB, SDR, or other group or individual.

REFERENCES

[1] S. D. Poisson, "Mémoire sur la propagation du mouvement dans les milieux élastiques," Mémoires de l'Académie des Sci. de l'Institut de France, 1831, pp. 549–606, vol. 10.

[2] J. A. Hunter et al., "Seismic site characterization with shear wave (SH) reflection and refraction methods," *J. Seismol.*, vol. 26, no. 4, pp. 631–652, Aug. 2022.

[3] Y. Wang et al., "Plane stress measurement on the cross-section of steel components using ultrasonic shear waves," *Mech. Syst. Signal Process.*, vol. 191, May 2023, Art. no. 110185.

[4] S. Lin, X. Tang, H.-N. Li, N. Gucunski, and Y. Wang, "Nondestructive evaluation of concrete compressive strength using shear-horizontal waves," *J. Perform. Constructed Facilities*, vol. 37, no. 1, Feb. 2023, Art. no. 06022002.

[5] A. J. Dawson, J. E. Michaels, J. W. Kummer, and T. E. Michaels, "Quantification of shear wave scattering from far-surface defects via ultrasonic wavefield measurements," *IEEE Trans. Ultrason., Ferroelectr., Freq. Control*, vol. 64, no. 3, pp. 590–601, Mar. 2017.

[6] A. P. Sarvazyan, O. V. Rudenko, S. D. Swanson, J. B. Fowlkes, and S. Y. Emelianov, "Shear wave elasticity imaging: A new ultrasonic technology of medical diagnostics," *Ultrasound Med. Biol.*, vol. 24, no. 9, pp. 1419–1435, Dec. 1998.

[7] K. Nightingale, M. S. Soo, R. Nightingale, and G. Trahey, "Acoustic radiation force impulse imaging: In vivo demonstration of clinical feasibility," *Ultrasound Med. Biol.*, vol. 28, no. 2, pp. 227–235, Feb. 2002.
[8] K. Nightingale, S. McAleavey, and G. Trahey, "Shear-wave generation using acoustic radiation force: In vivo and ex vivo results," *Ultrasound Med. Biol.*, vol. 29, no. 12, pp. 1715–1723, Dec. 2003.
[9] J. Bercoff, M. Tanter, and M. Fink, "Supersonic shear imaging: A new technique for soft tissue elasticity mapping," *IEEE Trans. Ultrason., Ferroelectr., Freq. Control*, vol. 51, no. 4, pp. 396–409, Apr. 2004.
[10] I. Z. Nenadic, M. W. Urban, J. F. Greenleaf, J. L. Gennisson, M. Bernal, and M. Tanter, *Ultrasound Elastography for Biomedical Applications and Medicine*. Hoboken, NJ, USA: Wiley, 2019.
[11] J. F. Greenleaf, M. Fatemi, and M. Insana, "Selected methods for imaging elastic properties of biological tissues," *Annu. Rev. Biomed. Eng.*, vol. 5, no. 1, pp. 57–78, Aug. 2003.
[12] Z. Zhang et al., "Noninvasive measurement of local stress inside soft materials with programmed shear waves," *Sci. Adv.*, vol. 9, no. 10, Mar. 2023, Art. no. eadd4082.
[13] L. Knopoff, "Scattering of shear waves by spherical obstacles," *Geophysics*, vol. 24, pp. 209–219, Apr. 1959.
[14] N. G. Einspruch, E. J. Witterholt, and R. Truell, "Scattering of a plane transverse wave by a spherical obstacle in an elastic medium," *J. Appl. Phys.*, vol. 31, pp. 806–818, Jun. 1960.
[15] D. W. Kraft and M. C. Franzblau, "Scattering of elastic waves from a spherical cavity in a solid medium," *J. Appl. Phys.*, vol. 42, no. 8, pp. 3019–3024, Jul. 1971.
[16] R. J. McBride and D. W. Kraft, "Scattering of a transverse elastic wave by an elastic sphere in a solid medium," *J. Appl. Phys.*, vol. 43, no. 12, pp. 4853–4861, Dec. 1972.
[17] Y. Iwashimizu, "Scattering of shear waves by an elastic sphere embedded in an infinite elastic solid," *J. Sound Vib.*, vol. 40, no. 2, pp. 267–271, May 1975.
[18] D. L. Jain and R. P. Kanwal, "Scattering of acoustic, electromagnetic and elastic SH waves by two-dimensional obstacles," *Ann. Phys.*, vol. 91, pp. 1–39, May 1975.
[19] D. L. Jain and R. P. Kanwal, "Scattering of P and S waves by spherical inclusions and cavities," *J. Sound Vib.*, vol. 57, no. 2, pp. 171–202, Mar. 1978.
[20] R. Lim and R. H. Hackman, "A parametric analysis of attenuation mechanisms in composites designed for echo reduction," *J. Acoust. Soc. Amer.*, vol. 87, no. 3, pp. 1076–1103, Mar. 1990.
[21] V. A. Korneev and L. R. Johnson, "Scattering of *P* and *S* waves by a spherically symmetric inclusion," *Pure Appl. Geophys.*, vol. 147, no. 4, pp. 675–718, Oct. 1996.
[22] A. Maurel, J.-F. Mercier, and F. Lund, "Scattering of an elastic wave by a single dislocation," *J. Acoust. Soc. Amer.*, vol. 115, no. 6, pp. 2773–2780, Jun. 2004.
[23] S. K. Kanaun and V. M. Levin, "Propagation of shear elastic waves in composites with a random set of spherical inclusions (effective field approach)," *Int. J. Solids Struct.*, vol. 42, no. 14, pp. 3971–3997, Jul. 2005.
[24] G. F. Wang, "Diffraction of shear waves by a nanosized spherical cavity," *J. Appl. Phys.*, vol. 103, no. 5, Mar. 2008, Art. no. 053519.
[25] X. Liu, S. Greenhalgh, and B. Zhou, "Scattering of plane transverse waves by spherical inclusions in a poroelastic medium," *Geophys. J. Int.*, vol. 176, no. 3, pp. 938–950, Mar. 2009.
[26] S. G. Haslinger, M. J. S. Lowe, P. Huthwaite, R. V. Craster, and F. Shi, "Elastic shear wave scattering by randomly rough surfaces," *J. Mech. Phys. Solids*, vol. 137, Apr. 2020, Art. no. 103852.
[27] G. C. Gaunaurd and H. M. Überall, "Deciphering the scattering code contained in the resonance echoes from fluid-filled cavities in solids," *Science*, vol. 206, no. 4414, pp. 61–64, Oct. 1979.
[28] G. C. Gaunaurd, "Transient and steady state scattering of acoustic waves from elastic objects in fluids and of elastic waves from inclusions in solid media: Direct and inverse scattering aspects," *J. Sound Vib.*, vol. 159, no. 3, pp. 421–440, Dec. 1992.
[29] D. Brill, G. Gaunaurd, and H. Überall, "Resonance theory of elastic shear-wave scattering from spherical fluid obstacles in solids," *J. Acoust. Soc. Amer.*, vol. 67, pp. 414–424, Feb. 1980.
[30] D. Brill and G. Gaunaurd, "Resonance theory of elastic waves ultrasonically scattered from an elastic sphere," *J. Acoust. Soc. Amer.*, vol. 81, no. 1, pp. 1–21, Jan. 1987.
[31] P. M. Morse and H. Feshbach, *Methods of Theoretical Physics*, vol. 2. New York, NY, USA: McGraw-Hill, 1953.
[32] F. G. Mitri, "Radiation force of stationary elastic compressional and shear plane waves on a cylinder encased in a linear elastic solid," *Forces Mech.*, vol. 4, Oct. 2021, Art. no. 100040.
[33] F. G. Mitri, "Acousto-elastic radiation force on a fluid cylindrical inclusion embedded in a linear elastic medium," *Chin. J. Phys.*, vol. 77, pp. 1843–1853, Jun. 2022.
[34] T. H. Tan, "Theorem on the scattering and the absorption cross section for scattering of plane, time-harmonic, elastic waves," *J. Acoust. Soc. Amer.*, vol. 59, no. 6, pp. 1265–1267, Jun. 1976.
[35] F. G. Mitri, "Extinction efficiency of 'elastic–sheet' beams by a cylindrical (viscous) fluid inclusion embedded in an elastic medium and mode conversion—Examples of nonparaxial Gaussian and Airy beams," *J. Appl. Phys.*, vol. 120, Oct. 2016, Art. no. 144902.
[36] P. J. Westervelt, "The theory of steady forces caused by sound waves," *J. Acoust. Soc. Amer.*, vol. 23, no. 3, pp. 312–315, May 1951.
[37] P. J. Westervelt, "Acoustic radiation pressure," *J. Acoust. Soc. Amer.*, vol. 29, no. 1, pp. 26–29, Jan. 1957.
[38] H. Olsen, W. Romberg, and H. Wergeland, "Radiation force on bodies in a sound field," *J. Acoust. Soc. Amer.*, vol. 30, no. 1, pp. 69–76, Jan. 1958.
[39] F. G. Mitri, "Acoustic backscattering and radiation force on a rigid elliptical cylinder in plane progressive waves," *Ultrasonics*, vol. 66, pp. 27–33, Mar. 2016.
[40] J. P. Leão-Neto, J. H. Lopes, and G. T. Silva, "Extended optical theorem in isotropic solids and its application to the elastic radiation force," *J. Appl. Phys.*, vol. 121, no. 14, Apr. 2017, Art. no. 144902.
[41] S. Chen, M. Fatemi, and J. F. Greenleaf, "Quantifying elasticity and viscosity from measurement of shear wave speed dispersion," *J. Acoust. Soc. Amer.*, vol. 115, no. 6, pp. 2781–2785, Jun. 2004.
[42] F. G. Mitri, "Radiation force of compressional plane waves on a sphere embedded in an elastic medium," *Forces Mech.*, vol. 12, Aug. 2023, Art. no. 100221.
[43] F. Liu and Z. Liu, "Elastic waves scattering without conversion in metamaterials with simultaneous zero indices for longitudinal and transverse waves," *Phys. Rev. Lett.*, vol. 115, no. 17, Oct. 2015, Art. no. 175502.
[44] O. Ordeig, S. Y. Chin, S. Kim, P. V. Chitnis, and S. K. Sia, "An implantable compound-releasing capsule triggered on demand by ultrasound," *Sci. Rep.*, vol. 6, Mar. 2016, Art. no. 22803.
[45] K. K. Ahmed, M. A. Tamer, M. M. Ghareeb, and A. K. Salem, "Recent advances in polymeric implants," *AAPS PharmSciTech*, vol. 20, no. 7, Oct. 2019, Art. no. 300.
[46] B. M. G. Rosa and G.-Z. Yang, "Ultrasound powered implants: Design, performance considerations and simulation results," *Sci. Rep.*, vol. 10, no. 1, Apr. 2020, Art. no. 6537.
[47] B. Gil, S. Anastasova, and G.-Z. Yang, "Low-powered implantable devices activated by ultrasonic energy transfer for physiological monitoring in soft tissue via functionalized electrochemical electrodes," *Biosensors Bioelectron.*, vol. 182, Jun. 2021, Art. no. 113175.
[48] T. Kubiak, M. Zubko, and A. Józefczak, "Ultrasound-triggered directional release from turmeric capsules," *Particuology*, vol. 57, pp. 19–27, Aug. 2021.
[49] F. G. Mitri, R. X. Li, and H. Sun, "Optical radiation force on a perfect electromagnetic conductor (PEMC) sphere," *J. Quant. Spectrosc. Radiat. Transf.*, vol. 256, Nov. 2020, Art. no. 107280.
[50] F. G. Mitri, "Optical trapping of a perfect electromagnetic conductor (PEMC) sphere exhibiting rotary polarization using nonparaxial focused Gaussian single-beam tweezers," *Results Opt.*, vol. 4, Aug. 2021, Art. no. 100089.
[51] F. G. Mitri, H. Tang, R. Li, and S. Gong, "Interaction of circularly polarized light with an absorptive electromagnetic conductor sphere—Radiation force and spin torque," *Results Opt.*, vol. 5, Dec. 2021, Art. no. 100128.
[52] F. G. Mitri, "Optical TM $\rightleftarrows$ TE mode conversion contribution to the radiation force on a cylinder exhibiting rotary polarization in circularly polarized light," *J. Quant. Spectrosc. Radiat. Transf.*, vol. 253, Sep. 2020, Art. no. 107115.